

NEW DISPERSION MODEL OF THE OPTICAL CONSTANTS OF THE DLC FILMS *

Daniel Franta^{1*}, Lenka Zajičková^{*†}, Vilma Buršíková^{*}, Ivan Ohlídal[†]

* *Laboratory of Plasma Physics and Plasma Sources, Faculty of Science, Masaryk University, Kotlářská 2, 611 37 Brno, Czech Republic,*

† *Department of Physical Electronics, Faculty of Science, Masaryk University, Kotlářská 2, 611 37 Brno, Czech Republic*

Received 14 April 2003 in final form 26 May 2003, accepted 28 May 2003

In this paper a new dispersion model of the optical constants of amorphous solids enabled us to perform an efficient parameterization of the optical constants of diamond like carbon (DLC) thin films. The model was based on the mathematical modeling of the density of electronic states (DOS) corresponding to both the valence and conduction bands. Moreover, the existence of the σ and π electronic states was taken into account, i. e. two valence and two conduction bands were supposed. The imaginary and real parts of the dielectric function were then calculated by the numerical convolution of the DOS and using a corresponding Kramers–Kronig relation, respectively. According to the model the DOS as well as the optical constants were calculated from ellipsometric measurements in the range 240–830 nm and estimated even outside this range. From the parameters of the model we evaluated also the ratio of π -to- σ electrons and consequently the sp^3 -to- sp^2 ratio using a known hydrogen atomic fraction. The optical constants of DLC films with addition of SiO_x were determined and compared with DLC too.

PACS: 78.20.Bh, 78.20.Ci, 78.66.Jg

1 Introduction

The investigation of diamond like carbon (DLC) films has been already attracted much attention because of their unique properties such as high mechanical hardness, low friction, high thermal conductivity, inertness against corrosive gases, transparency in the visible and IR spectral region and low electron affinity (see e. g. [1–4]). Previously, we have determined spectral dependences of the optical constants of the DLC films without any parameterization in the range 240–830 nm by a multi-sample modification of variable angle spectroscopic ellipsometry (VASE) [5]. In the same paper the spectral dependences of the determined optical constants were interpreted using a dispersion model based on two modified Lorentz oscillators corresponding to both $\pi \rightarrow \pi^*$ and $\sigma \rightarrow \sigma^*$ interband transitions. In Ref. [6] we have shown that a new dispersion model based on mathematical modeling of the density of electronic states (DOS) corresponding to both the valence and conduction bands can be successfully used for the optical constants of amorphous

*Presented at XIVth Symposium on Application of Plasma Processes, Liptovský Mikuláš (Slovakia), January 2003.

¹E-mail address: franta@physics.muni.cz

solids, particularly for chalcogenide films. Since DLC films consist of sp^3 and sp^2 bonded carbon, four σ electrons in sp^3 site carbon and three σ and one π electrons in sp^2 site carbon can be found [7]. In the present work we extended the above DOS model to the DLC films taking into account the existence of both, the π and σ electronic states. By this way we constructed a Kramers–Kronig consistent model of optical constants of DLC working in a wide spectral range.

Moreover, we used the same model for DLC films deposited with an addition of SiO_x groups (denoted as DLC: SiO_x films). Motivation for a study of modified DLC films, such as DLC: SiO_x , consists in a relatively strong intrinsic stress of pure DLC films which represents a certain disadvantage for their practical applications [8, 9]. This fact namely causes a peeling of the films and limits considerably a deposition of relatively thick films. It was found that the intrinsic stress in the DLC: SiO_x films prepared by plasma enhanced chemical vapor deposition (PECVD) from a mixture of methane (CH_4) and hexamethyldisiloxane ($C_6H_{18}Si_2O$, the abbreviation of this material is HMDSO) was strongly reduced [10–12]. In Ref. [12] a complex characterisation of DLC: SiO_x was performed including modeling of optical constants in the range restricted to 400–830 nm. The model used was a Cauchy formula for refractive index and an exponential form of extinction coefficient. Obviously, this model was not Kramers–Kronig consistent. Anyway, it has been shown that DLC: SiO_x films exhibited, besides improved mechanical properties, slightly different optical properties as compared with DLC. In the present paper, we compared DLC: SiO_x optical constants obtained in the whole measured range, 240–830 nm, using a Kramer–Kronig consistent model with these of pure DLC.

2 Description of the dispersion model

The model was created on the basis of the following assumptions:

- The real and imaginary parts of the dielectric function fulfill the Kramers–Kronig relations.
- The dielectric function is odd with regard to photon energy E ($\varepsilon_2(-E) = -\varepsilon_2(E)$), i. e. symmetrical to time-reversal.
- The σ and π bonding states form the two σ and π valence bands. Similarly, the excited σ^* and π^* antibonding states form the two σ^* and π^* conduction bands.
- The absorption is caused by interband transitions between the $\sigma \rightarrow \sigma^*$ and $\pi \rightarrow \pi^*$ states. The DOS distribution is parabolic as in crystals in the vicinity of the energy extrema of both the valence and conduction bands [13].
- Transitions $\sigma \rightarrow \pi^*$ and $\pi \rightarrow \sigma^*$ are considerably less probable than transitions $\sigma \rightarrow \sigma^*$ and $\pi \rightarrow \pi^*$ and therefore can be neglected.
- For simplicity, the DOS is symmetrical with respect to the Fermi energy E_F ($E_F = 0$).

The above assumptions on the DOS distribution for DLC films are demonstrated in Fig. 1. It is evident that in the model there are low and high energy limits of both, the $\sigma \rightarrow \sigma^*$ and $\pi \rightarrow \pi^*$ transitions, i. e. $E_{g\sigma}$, $E_{h\sigma}$, $E_{g\pi}$ and $E_{h\pi}$. The DOS distribution of the valence bands $N_{vj}(E)$

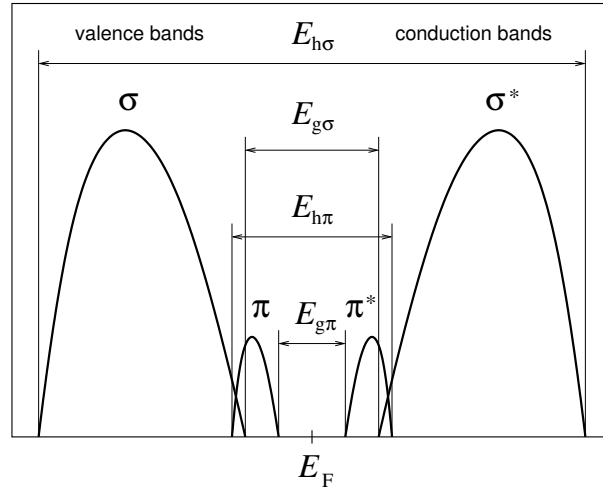


Fig. 1. The schematic diagram of the DOS distribution for the DLC.

(where $j = \sigma, \pi$) can be expressed as

$$N_{vj}(E) = \begin{cases} A_j \sqrt{-E - \frac{E_{gj}}{2}} \sqrt{\frac{E_{hj}}{2} + E}, & -\frac{E_{hj}}{2} < E < -\frac{E_{gj}}{2} \\ 0, & \text{otherwise.} \end{cases} \quad (1)$$

The parameter A_j is proportional to the valence σ and π electron densities of the material. One can symmetrically express the DOS for the conduction bands:

$$N_{cj}(E) = \begin{cases} A_j \sqrt{E - \frac{E_{gj}}{2}} \sqrt{\frac{E_{hj}}{2} - E}, & \frac{E_{gj}}{2} < E < \frac{E_{hj}}{2} \\ 0, & \text{otherwise.} \end{cases} \quad (2)$$

The contribution of $\sigma \rightarrow \sigma^*$ and $\pi \rightarrow \pi^*$ transitions to the imaginary part of the dielectric function can be calculated as a convolution of the valence and conduction DOS distributions [13]:

$$\varepsilon_{2j}(E) = \left(\frac{2\pi e\hbar}{mE} \right)^2 \frac{(2\pi)^3}{2} \frac{1}{\mathcal{B}_0} |p_{vc,j}|^2 \int_{-\infty}^{\infty} N_{vj}(S) N_{cj}(S+E) dS, \quad (3)$$

where e , \hbar , m , \mathcal{B}_0 and $|p_{vc,j}|^2$ are electron charge, Planck's constant, electron mass, certain part of the Brillouin zone of the corresponding crystalline material and squared momentum-matrix element, respectively. All the constants in front of the integral can be included into the constant A_j . Then the total imaginary part of the dielectric function has a simple sum form:

$$\varepsilon_2(E) = \sum_{j=\sigma,\pi} \frac{1}{E^2} \int_{-\infty}^{\infty} N_{vj}(S) N_{cj}(S+E) dS, \quad (4)$$

where the symbols $N_{v\sigma}(E)$, $N_{c\sigma}(E)$, $N_{v\pi}(E)$ and $N_{c\pi}(E)$ now represent the quantities proportional to the DOS distribution in the corresponding bands.

The corresponding real part of the dielectric function is expressed by the Kramers–Kronig relation [14] as:

$$\varepsilon_1(E) = 1 + \frac{2}{\pi} \int_0^{\infty} \frac{S \varepsilon_2(S)}{S^2 - E^2} dS. \quad (5)$$

The integral Eq. (5) can be transformed into numerically more convenient form using the time-reversal symmetry and a suitable substitution:

$$\varepsilon_1(E) = 1 + \frac{1}{\pi} \int_0^1 \frac{\varepsilon_2(E + \frac{x}{1-x}) - \varepsilon_2(E - \frac{x}{1-x})}{x(1-x)} dx. \quad (6)$$

The *six-parameter dispersion model* of the dielectric function $\hat{\varepsilon}(E) = \varepsilon_1(E) + i\varepsilon_2(E)$ of the amorphous carbon materials is based on Eqs. (1), (2), (4) and (6). The parameters characterizing the model are A_σ , $E_{g\sigma}$, $E_{h\sigma}$, A_π , $E_{g\pi}$ and $E_{h\pi}$.

3 Preparation of the samples

The DLC and DLC:SiOx films were prepared by PECVD method in r. f. low pressure glow discharges. The reactor chamber was a glass cylinder closed by two stainless steel flanges and evacuated by a diffusion pump. The bottom graphite electrode, on which the substrates for deposition were placed, was capacitively coupled to a generator working at the frequency of 13.56 MHz. The upper graphite electrode, 100 mm in the diameter, was 55 mm apart from the bottom electrode of the 148 mm in diameter. A detailed description of the reactor is given in Ref. [15]. The pressure in the reactor was measured with an absolute vacuum manometer (Capacitron Leybold). The depositions were carried out in the flow regime and the flow rates of gases were controlled by Hastings electronic flow controllers.

All the depositions were carried out at the r. f. power of 100 W. DLC films were deposited from a mixture of methane (CH_4) and argon. The dc negative self-bias -400 V due to the capacitive coupling and different mobility of electrons and ions occurred on the r. f. driven electrode. The flow rate of methane (Q_{CH_4}) was 1.3 sccm and the corresponding partial pressure was $p_{\text{CH}_4} = 5.6$ Pa. The flow rate of argon (Q_{Ar}) was 0.3 sccm with the partial pressure $p_{\text{Ar}} = 3.6$ Pa. We kept constant all the deposition conditions except the deposition time that varied from 5 to 90 min. By this way we obtained similar films which thicknesses varied in the range 35–510 nm.

In case of the DLC:SiOx film depositions the HMDSO monomer was added into the CH_4/Ar gas feed. Here, the dc negative bias was -350 V. The flow rates of CH_4 , Ar and HMDSO were 1.4, 0.35 and 0.25 sccm, respectively. The total pressure was 9.8 Pa. As above we changed the deposition time in order to obtain films with different thicknesses. The depositions lasted from 5 to 50 min which corresponded to the thicknesses in the range 160–700 nm.

4 Data acquisition and processing

Ellipsometric measurements of the films deposited on silicon substrates were performed in the spectral range from 240 to 830 nm (1.5–5.2 eV). The angle of incidence varied from 55° to 75° in steps of 5°. A UVISSEL DH10 Jobin-Yvon phase-modulated ellipsometer was used to measure the ellipsometric quantities in the reflection mode using zone averaging (for details see Ref. [5]). By this procedure we obtained relatively precise spectral dependences of the ellipsometric ratio $\hat{\rho}$ characterizing the film-substrate system as well as an estimation of its errors. The ellipsometric ratio $\hat{\rho}$ is defined as

$$\hat{\rho} = \frac{\hat{r}_p}{\hat{r}_s} \quad (7)$$

where \hat{r}_p and \hat{r}_s represent the Fresnel coefficients of the samples. These coefficients are a function of optical parameters of the system under study (see below).

We applied a multi-sample modification of variable angle spectroscopic ellipsometry (VASE) method for determining the parameters of the prepared films. Within this method all the data measured on a whole set of the films, either DLC or DLC:SiO_x, were treated simultaneously under assumption that every particular set of the films is formed by the same material from the optical point of view. This means that either DLC or DLC:SiO_x differed only in thicknesses. For more details on the multi-sample methods, in general, refer to Ref. [16]. In particular, we assumed a model of a homogeneous isotropic film on a homogeneous isotropic substrate. Optical constants of the silicon substrate were taken from Ref. [17]. The layers were characterized by spectral dependences of the refractive index n_f , extinction coefficient k_f and by their thickness d_f . Further, we can write

$$\hat{n}_f = n_f - i k_f = \sqrt{\varepsilon^*} \quad (8)$$

where ε^* is complex conjugated² film dielectric function defined by our six-parameters model (see sec. 2). These six parameters together with the film thicknesses have been found by a least-squares method (LSM) constructing the following merit function:

$$S(\vec{X}) = \sum_k |\hat{\rho}(\vec{X}, \lambda_k, \theta_{0k}) - \hat{\rho}_k^{\text{exp}}|^2 w_k \quad (9)$$

where \vec{X} denotes the vector whose components are identical with the parameters sought and $\hat{\rho}_k^{\text{exp}}$ are the experimental values. Subscript k counts for the measurements, w_k and λ_k are the weight of the experimental values and the wavelengths, respectively, and θ_{0k} is the angle of incidence of light falling onto the upper boundary of the system. The theoretical values $\hat{\rho}(\vec{X}, \lambda_k, \theta_{0k})$ were calculated using a matrix formalism [18, 19]. For searching the best fit, i. e. the minimum of $S(\vec{X})$, the Marquardt–Levenberg algorithm was applied [20].

5 Results and discussion

In Figs. 2 and 3 the selected real and imaginary parts of the measured ellipsometric ratio $\hat{\rho}$ are compared with the corresponding theoretical values. The theoretical values are calculated on

²Complex conjugation resulted formally from the definition of the ellipsometric ratio $\hat{\rho}$.

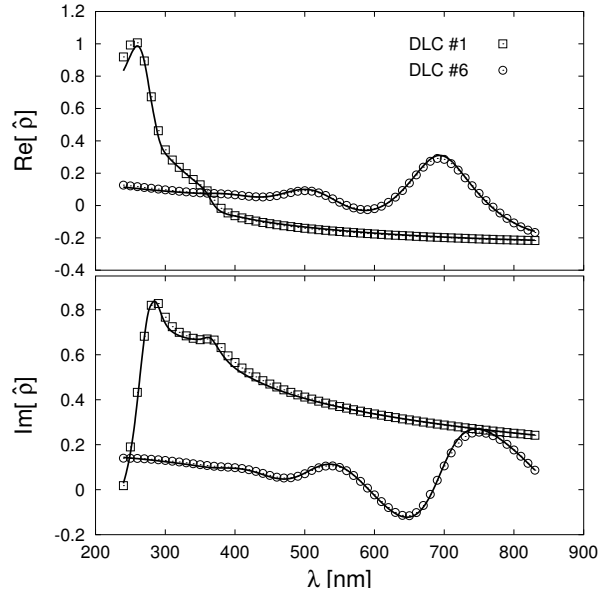


Fig. 2. Spectral dependences of real and imaginary parts of the ellipsometric ratio $\hat{\rho}$ for two selected DLC films and 65° angle of incidence. Points and curves represent experimental and theoretical values, respectively. Film labels are given in the figure legend and correspond to thicknesses given in Table 1.

the basis of the best fits. We can see that the agreement between the measured and theoretical values is good. Parameters of the films and their statistical errors obtained from the best fits are summarized in Table 1. All the six parameters of the model were searched during the fits I. and II. However, in case of DLC:SiO_x the parameters $E_{h\sigma}$ and $E_{h\pi}$ had very high errors and their correlation coefficient was equal to one. This means they could not be determined independently. Therefore we decided to perform a new fit, labeled III., in which they were merged in one parameter, i. e. the optical constants were described by the five-parameter model. A physical reason why these two parameters had to be merged is the fact that the high energy limits of both transitions are far from the upper energy 5.2 eV at which the ellipsometric ratio could be measured. Note that high energy interband transitions ($E \gg 5.2$ eV) contribute only to the real part of the dielectric function in the measured range by an additive constant.³ From Table 1 we can see that both fits II. and III. give practically the same values of the parameters. Since the parameters in the fit III. are not correlated their statistical errors are reduced.

The optical constants corresponding to the fits I. and III. are depicted for the measured spectral range in Fig. 4. In fact, the optical constants belonging to the fit III. could represent also the results of the fit II. The atomic composition of the films obtained by Rutherford backscattering spectroscopy show that even 7.8 % additional SiO_{0.24} groups change significantly the optical

³Most of the other models describe the high energy transitions simply by using parameter $\varepsilon_{1\infty}$, e. g. Jellison–Modine model [21]. In contrary, this parameter does not exist in our model and therefore the high energy limit of $\hat{\varepsilon}$ has a correct value of vacuum ($\hat{\varepsilon}(\infty) = 1$).

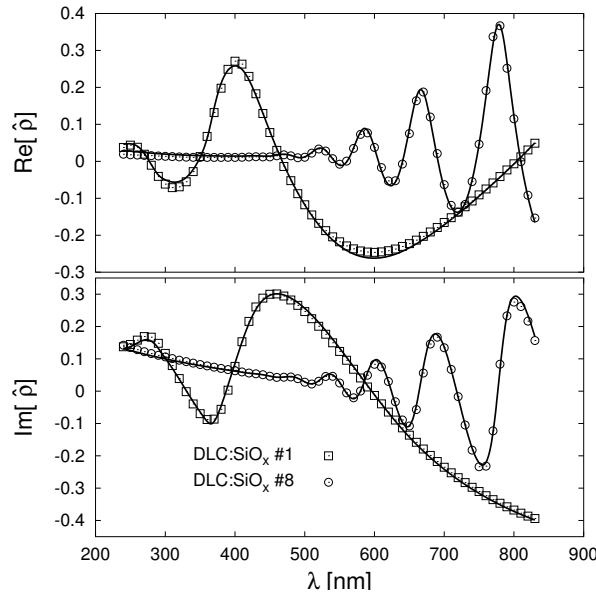


Fig. 3. Spectral dependences of real and imaginary parts of the ellipsometric ratio $\hat{\rho}$ for two selected DLC:SiO_x films and 65° angle of incidence. Points and curves represent experimental and theoretical values, respectively. Film labels are given in the figure legend and correspond to thicknesses given in Table 1.

properties of the films. The refractive index of the DLC:SiO_x films is higher than in case of the DLC films. This means that the total density of valence electrons is higher and/or the DOS distribution is moved to lower energies. On the other hand, the extinction coefficient in the visible is lower for the DLC:SiO_x films and we cannot observe a resolved absorption peak of $\pi \rightarrow \pi^*$ electron transitions.

From the parameters obtained within our model we can of course construct the dielectric function of both materials studied as well as the distribution of DOS in a wide energy range (see Figs. 5 and 6). It should be noticed, however, that it is only a certain estimation of the material optical response outside the measured range that is depicted by two vertical lines in Fig. 5. In Fig. 6 the curves plotted represent the quantities $N_{v\sigma}(E)$, $N_{c\sigma}(E)$, $N_{v\pi}(E)$ and $N_{c\pi}(E)$ proportional to the DOS distribution of the films. The normalized DOS distribution can be obtained by a normalization of the sum $N(E) = N_{v\sigma}(E) + N_{v\pi}(E)$ and multiplying by the factor equal to the density of the valence electrons. The advantage of the model is the separation of optical responses from σ and π electron transitions. According to the following formula we calculated quantities proportional to the density \mathcal{N}_j of both the electrons ($j = \pi, \sigma$)

$$\mathcal{N}_j \propto A_j(E_{hj} - E_{gj})^2 \quad (10)$$

and obtained the relative densities of σ and π electrons for DLC films, 96.9 % and 3.1 %, respectively. The DLC films are composed of carbon in sp^3 and sp^2 configurations and hydrogen. Four

Tab. 1. Six parameters characterizing the optical properties of the DLC and DLC:SiO_x films and the thicknesses of these films found by fitting the measured ellipsometric ratio.

	DLC fit I.	DLC:SiO _x fit II.	DLC:SiO _x fit III.
A_σ [eV ^{-1/2}]	0.484 ± 0.004	0.54 ± 0.11	0.545 ± 0.003
$E_{g\sigma}$ [eV]	1.613 ± 0.005	1.901 ± 0.005	1.897 ± 0.005
$E_{h\sigma}$ [eV]	56.6 ± 0.5	46 ± 20	46.3 ± 0.3
A_π [eV ^{-1/2}]	0.946 ± 0.008	0.39 ± 0.16	0.387 ± 0.003
$E_{g\pi}$ [eV]	0.837 ± 0.006	1.170 ± 0.005	1.168 ± 0.003
$E_{h\pi}$ [eV]	7.88 ± 0.06	46 ± 37	$E_{h\pi} \equiv E_{h\sigma}$
d_{f1} [nm]	34.94 ± 0.03	160.93 ± 0.08	160.93 ± 0.08
d_{f2} [nm]	72.38 ± 0.03	266.56 ± 0.11	266.56 ± 0.11
d_{f3} [nm]	111.82 ± 0.05	412.12 ± 0.18	412.10 ± 0.18
d_{f4} [nm]	242.72 ± 0.09	489.16 ± 0.19	489.15 ± 0.19
d_{f5} [nm]	335.37 ± 0.14	576.4 ± 0.3	576.4 ± 0.3
d_{f6} [nm]	510.05 ± 0.19	706.4 ± 0.3	706.3 ± 0.3
d_{f7} [nm]	–	892.2 ± 0.3	892.2 ± 0.3
d_{f8} [nm]	–	1185.8 ± 0.5	1185.8 ± 0.5

σ electrons belong to sp³ site carbon, three σ and one π electrons to sp² site carbon and each hydrogen atom contributes to a single σ electron. Then, we can write

$$\begin{aligned} \mathcal{N}_\pi &= \mathcal{N}_{C(sp^2)} \\ \mathcal{N}_\sigma &= \mathcal{N}_H + 4\mathcal{N}_{C(sp^3)} + 3\mathcal{N}_{C(sp^2)} \\ 1 &= \mathcal{N}_H + \mathcal{N}_{C(sp^3)} + \mathcal{N}_{C(sp^2)} \end{aligned}$$

where \mathcal{N}_H , $\mathcal{N}_{C(sp^3)}$ and $\mathcal{N}_{C(sp^2)}$ are atomic fractions of hydrogen, sp³ and sp² bonded carbon, respectively and \mathcal{N}_σ , \mathcal{N}_π are fractions of σ , π electrons per one atom, respectively. The optical, electrical and mechanical properties of the DLC films appeared to be determined by the relative amounts of sp³ and sp² sites. Since we know the ratio of π -to- σ electrons from our model and the atomic fraction of hydrogen from elastic recoil detection analysis (ERDA) we can easily found the sp³-to-sp² ratio similar as in Ref. [22] using Eq. (11):

$$\frac{\mathcal{N}_{C(sp^3)}}{\mathcal{N}_{C(sp^2)}} = \frac{(1 - 3\alpha) - \mathcal{N}_H(1 - 2\alpha)}{\alpha(4 - 3\mathcal{N}_H)} \quad (11)$$

where

$$\alpha = \frac{\mathcal{N}_\pi}{\mathcal{N}_\sigma} = \frac{A_\pi(E_{h\pi} - E_{g\pi})^2}{A_\sigma(E_{h\sigma} - E_{g\sigma})^2}. \quad (12)$$

Particularly, the hydrogen atomic fraction and the sp³-to-sp² ratio were 0.32 and 6.2 for the DLC films studied. These values classify the films as hard but possessing a relatively high internal

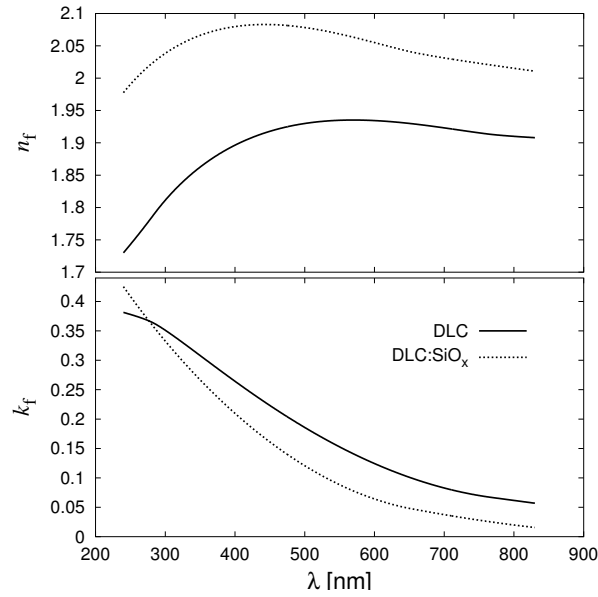


Fig. 4. The spectral dependences of both the refractive index n_f and extinction coefficient k_f of the DLC and DLC:SiO_x films.

stress [23]. This was confirmed also by the mechanical tests showing the hardness of the films as high as 24 GPa and a high compressive stress in the films causing their spontaneous delamination if the film thickness exceeded 0.6 μm [15].

In case of DLC:SiO_x films the same analysis cannot be performed. According to the Rutherford backscattering analysis (RBS) and ERDA the DLC:SiO_x are composed of 42 % carbon, 50 % hydrogen, 2 % oxygen and 6 % silicon. Therefore Eq. (11) is not strictly valid. If we neglect the contribution of silicon and oxygen bonds and use, nevertheless, above relations to estimate the ratio of π -to- σ electrons we get the value of 0.73. Such high amount of π electrons is not in agreement with the film high hardness of 20 GPa. Moreover, looking carefully at Fig. 6 we can see that the σ and π states are not as good separated as for DLC films. It means that these two bands do not represent σ and π electrons solely but rather more complicated structure of DLC:SiO_x that should be correctly described by more than two electron states. However, this would increase the number of fitting parameters above reasonable number resulting in a high correlations among them.

6 Conclusion

The formulae representing the dispersion model of optical constants of DLC films based on the parameterization of the DOS are described in detail. Within this parameterization the $\sigma \rightarrow \sigma^*$ and $\pi \rightarrow \pi^*$ interband transitions are respected. The dispersion model contains six parameters clearly characterizing DLC in a broad spectral range.

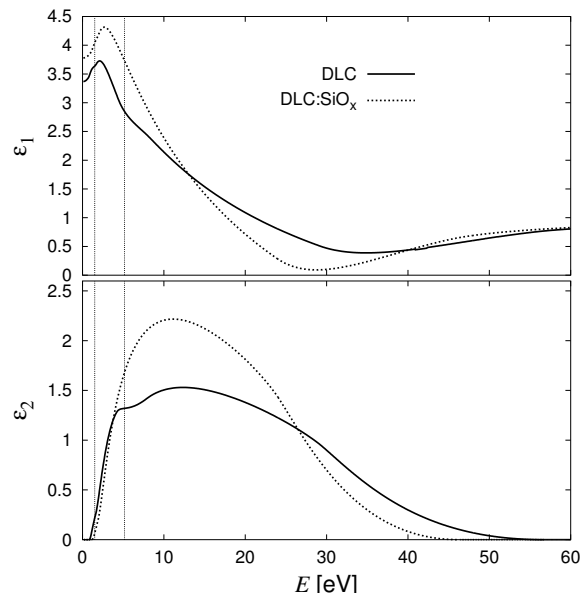


Fig. 5. The spectral dependences of real and imaginary parts of dielectric function of the DLC and DLC:SiO_x films calculated using the described dispersion model.

The model was successfully applied to interpret the ellipsometric measurements in the range 240–830 nm (1.5–5.2 eV) carried out on the DLC and DLC:SiO_x films with different thicknesses (multi-sample modification of VASE). The DOS as well as the optical constants were obtained in the measured range and could be estimated even outside this range using the model. In case of DLC films the ratio of π -to- σ electrons was evaluated simply from the model parameters found by fitting. Consequently, the sp^3 -to- sp^2 ratio was determined using this ratio and the known hydrogen atomic fraction. The optical constants of the DLC:SiO_x differed from these of pure DLC. In this case the two valence and two conduction bands do not represent σ and π electrons solely but rather more complicated structure of the films. Therefore we develop a new extended model for DLC:SiO_x.

Acknowledgement: This work was supported by the Grant Agency of the Czech Republic under contract 202/01/1110 and by the Ministry of Education of the Czech Republic under contracts MSM143100003, COST 527.20 and ME489. The numerical computations was performed using computers of the Supercomputing Center Brno.

References

- [1] A. Bubenzer, B. Dischler, G. Brandt, P. Koidl: *J. Appl. Phys.* **54** (1983) 4590
- [2] M. Alaluf, J. Appelbaum, L. Klibanov, D. Brinker, D. Scheiman, N. Croitoru: *Thin Solid Films* **256** (1995) 1

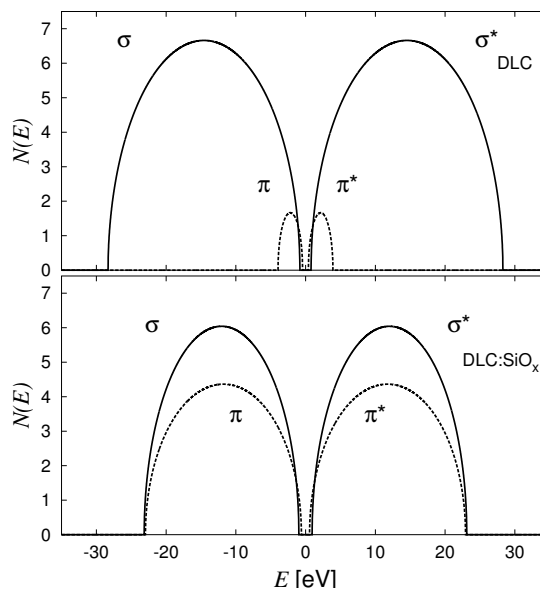


Fig. 6. The unnormalized DOS distribution of the DLC and DLC:SiO_x films calculated using the described dispersion model.

- [3] S. Egret, J. Robertson, W. I. Milne, F. J. Clough: *Diamond Relat. Mater.* **6** (1997) 879
- [4] D. P. Dowling, P. V. Kola, K. Donnelly, T. C. Kelly, K. Brumitt, L. Lloyd, R. Eloy, M. Therin, N. Weill: *Diamond Relat. Mater.* **6** (1997) 390
- [5] D. Franta, L. Zajíčková, I. Ohlídal, J. Janča, K. Veltruská: *Diamond Relat. Mater.* **11** (2002) 105
- [6] D. Franta, I. Ohlídal, M. Frumar, J. Jedelský: *Appl. Surf. Sci.* (2003) in print
- [7] J. Robertson: *Diamond Relat. Mater.* **6** (1997) 212
- [8] C. DeMartino, G. Fusco, G. Mina, A. Tagliaferro, L. Vanzetti, L. Calliari, M. Anderle: *Diamond Relat. Mater.* **6** (1997) 559
- [9] S. S. Camargo Jr., R. A. Santos, A. L. B. Neto, R. Carius, F. Finger: *Thin Solid Films* **332** (1998) 130
- [10] V. Buršíková, P. Sládek, P. Sťahel, L. Zajíčková: *J. Non-Cryst. Solids* **299** (2002) 1147
- [11] V. Buršíková, V. Navrátil, L. Zajíčková, J. Janča: *Mat. Sci. Eng. A* **324** (2002) 251
- [12] L. Zajíčková, V. Buršíková, V. Peřina, A. Macková, J. Janča: *Surf. Coatings Technol.* (2003) submitted
- [13] J. Tauc: *Optical Properties of Non-Crystalline Solids*, in: *Optical Properties of Solids* (Ed. F. Abelès) North-Holland, Amsterdam 1972, p. 291
- [14] L. de Kronig: *J. Opt. Soc. Am.* **12** (1926) 547
- [15] L. Zajíčková, V. Buršíková, D. Franta: *Czech. J. Phys.* **49** (1999) 1213
- [16] D. Franta, I. Ohlídal: *Acta Phys. Slovaca* **50** (2000) 411
- [17] C. M. Herzinger, B. Johs, W. A. McGahan, J. A. Woollam, W. Paulson: *J. Appl. Phys.* **83** (1998) 3323
- [18] I. Ohlídal, D. Franta: *Ellipsometry of Thin Film Systems*, in: *Progress in Optics*, vol. 41 (Ed. E. Wolf) Elsevier, Amsterdam 2000, pp. 181–282

- [19] I. Ohlídal, D. Franta: *Acta Phys. Slovaca* **50** (2000) 489
- [20] W. D. Marquardt: *J. Soc. Ind. Appl. Math.* **11** (1963) 431
- [21] G. E. Jellison Jr., F. A. Modine: *Appl. Phys. Lett.* **69** (1996) 371
- [22] F. Demichelis, C. F. Pirri, A. Tagliaferro: *Physical Review B* **45** (24) 1992 14364
- [23] W. Kulisch: *Deposition of Diamond-Like Superhard Materials* Springer-Verlag, Berlin 1999